Lewis number effects on partially premixed flames

By G. R. Ruetsch AND J. Ferziger

1. Motivation and objectives

Combustion is generally categorized as either premixed, where flames propagate into homogeneous mixtures of reactants, or as nonpremixed, where initially separated reactants diffuse into the reaction zones. Although these approaches are applicable to many combustion devices, there are cases not in either of these two limiting regimes. Under such circumstances, one must consider partially premixed combustion.

In partially premixed combustion, mechanisms from both premixed and nonpremixed regimes coexist and, as a result, some interesting phenomena arise. One such phenomenon is flame stabilization in laminar mixing layers by triple flames. These flames were first observed by Phillips (1965) in a methane mixing layer. Additional studies of triple flames are contained in Kioni *et al.* (1993), Dold (1989), Dold *et al.* (1991), Hartley and Dold 1991, Müller *et al.* (1994), and Ruetsch *et al.* (1995).

Triple flames may be thought of as an approach to partially premixed combustion from the nonpremixed limit. We can also approach the regime of partially premixed combustion from the premixed limit, where we consider inhomogeneously premixed flames. This regime has been addressed in Ruetsch and Broadwell (1995), where premixed flames were subjected to weak perturbations in mixture fraction.

One interesting feature of both triple and inhomogeneously premixed flames is the high curvature they possess. It is important to distinguish this type of curvature from that which arises from velocity fluctuations in the premixed case. Curvature of a flame due to velocity fluctuations is limited by various mechanisms which damp small wavenumber disturbances. In the partially premixed case, however, flame curvature is a consequence of the mixture fraction gradient which can be arbitrarily large. Aside from these geometrical aspects, this curvature plays a significant role in flame propagation. As an example, triple flames have propagation speeds that exceed the premixed flame speed by a factor of the square root of the density ratio. When the flames are confined laterally, as in the case of the inhomogeneously premixed flames, this mechanism for enhanced propagation speed due to heat release effects is greatly inhibited.

Another aspect of flame speed dependence on curvature is through the Lewis number, the ratio of thermal to mass diffusivities. This dependence of flame speed on the Lewis number relates to the thermal-diffusive instability, which has been extensively studied in the premixed case. Partially premixed combustion differs from the premixed case since the curvature in partially premixed cases can become very large and can be maintained by fixing the gradients in the approaching reactant field. This suggests that the partially premixed case provides a unique opportunity

to study Lewis number effects on flame speed. To this date, the topic of partially premixed combustion coupled with nonunity Lewis numbers has not been investigated. The present study addresses this issue.

We begin by reviewing the thermal-diffusive instability in premixed combustion and then discuss the configuration for studying similar behavior in the partially premixed case. This is followed by results of the numerical solutions and then by a set of model equations developed to evaluate and analyze the processes occurring in the simulations.

1.1 Thermal-diffusive instability

The thermal-diffusive instability is well documented for premixed flames (Williams 1986). Although we are considering partially premixed combustion, we expect and observe similarities with the premixed case. This thermal-diffusive mechanism relies on the strong influence of the temperature in the burnt gases on the reaction rate, and hence burning velocity. In turn, the temperature in the burnt gases increases with enhanced diffusion of reactant species into the flame and reduced diffusion of heat into the approaching flow. These diffusion rates are affected by the gradients in the species and temperature fields and by the values of the mass and thermal diffusivities. The ratio of the mass and thermal diffusivities is the Lewis number; the gradients in the profiles are modified by the differential diffusion of thermal energy and species. As a planar flame is perturbed slightly, the gradients of the reactant and temperature fields steepen or broaden. For unity Lewis number, the changes in mass and heat diffusion offset one another and the temperature in the burnt gases remains unchanged, as does the burning velocity. For Lewis numbers larger than unity, where the thermal diffusivity exceeds the mass diffusivity, the heat transfer out of the flame is dominant in the forward sections of the flame where the gradients are steeper. Likewise, the mass diffusion into the flame is dominant in the trough. This results in a stabilizing effect due to the temperature and burning velocity decreasing in the forward sections of the flame and increasing in the troughs. The opposite is true for Lewis numbers less than unity, where the flame becomes unstable to small perturbations.

1.2 Numerical simulation and flow configuration

We use direct numerical simulations to solve the fully compressible Navier-Stokes equations. The simulation uses a two-dimensional version of the code developed by Trouvé (1991). This code uses the high-order compact finite difference scheme of Lele (1992) for spatial differentiation, the third order Runge-Kutta scheme of Wray for time advancement, and the Navier-Stokes characteristic boundary conditions of Poinsot and Lele (1992). Below we summarize some of the important features and assumptions of the code relevant to this work; for further details on the numerical method readers are referred to Lele (1992) and Poinsot and Lele (1992).

The chemical scheme we consider is represented by a one-step global reaction between a fuel and oxidizer:

$$F + O \longrightarrow P$$

where we have assumed unity stoichiometric coefficients for simplicity. The reaction rate follows the Arrhenius form:

$$\dot{\omega} = K\rho Y_F \rho Y_O \exp\left(-\frac{T_{ac}}{T}\right)$$

where ρ is the density, T_{ac} is the activation temperature, K is the pre-exponential factor, and Y_F and Y_O are the fuel and oxidizer mass fractions. Following Williams (1986), we write this reaction rate as

$$\dot{\omega} = \Lambda\rho Y_F \rho Y_O \exp\left(-\frac{\beta(1-\theta)}{1-\alpha(1-\theta)}\right)$$

where the reduced pre-exponential factor (Λ), heat release parameter (α), Zel'dovich number (β), and reduced temperature (θ) are defined by:

$$\Lambda = K\exp(-\beta/\alpha); \quad \alpha = \frac{T_f - T_0}{T_f}; \quad \beta = \frac{\alpha T_{ac}}{T_f}; \quad \theta = \frac{T - T_0}{T_f - T_0}$$

with T_f being the adiabatic flame temperature and T_0 taken in the ambient flow. In this study we hold the Zel'dovich number constant at $\beta = 8$ and use a heat release parameter of $\alpha = 0.75$.

The transport coefficients in the simulations are temperature dependent. This temperature dependence is expressed through the molecular viscosity, μ, given by:

$$\mu = \mu_0 \left(\frac{T}{T_0}\right)^a$$

with $a = 0.76$. The temperature dependence of the thermal conductivity, λ, and the mass diffusivities, $\mathcal{D}_k$, is obtained by requiring the Lewis, Prandtl, and Schmidt numbers to be constant:

$$Le_k = \frac{\lambda}{\rho\mathcal{D}_k c_p}, \qquad Pr = \frac{\mu c_p}{\lambda}, \qquad Sc_k = \frac{\mu}{\rho\mathcal{D}_k}$$

where $k = F, O$ refers to the fuel or oxidizer species. Although we are concerned with variations in the Lewis number, we do not want to consider differential diffusion in this study. Therefore, we allow the Lewis number to vary from simulation to simulation, but require that all species have equal Lewis numbers. We modify the Lewis number by changing the mass diffusivity, or Schmidt number, while maintaining a constant thermal diffusivity in the cold gases. We also maintain constant planar premixed laminar flame speed by modifying the pre-exponential factor Λ.

We solve the compressible Navier-Stokes equations in the two-dimensional domain depicted in Fig. 1. At the boundaries in the horizontal direction we use an inflow boundary condition on the left and nearly-perfect reflective boundary conditions, required to avoid pressure drift, at the outflow. In the lateral direction, we use

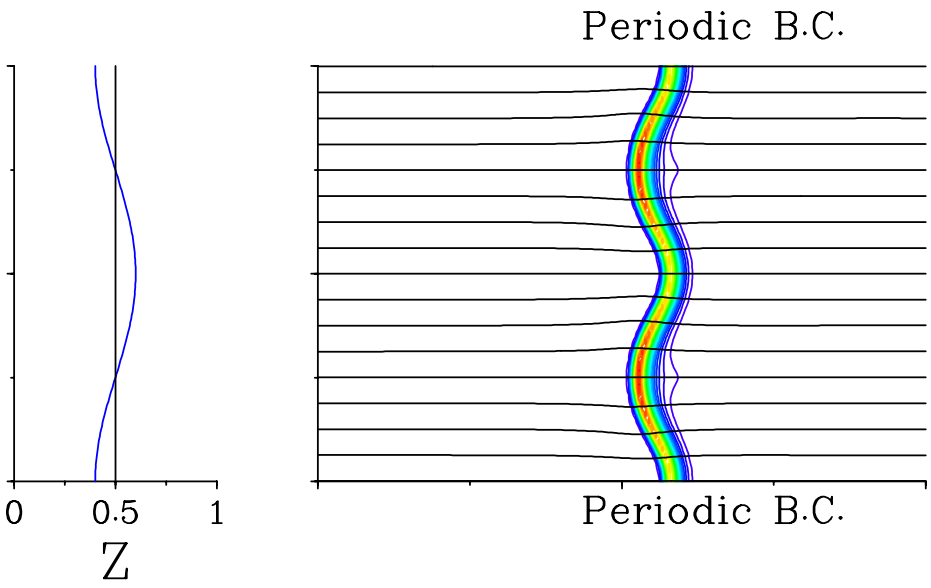

FIGURE 1. Computational domain used in the simulations. The left boundary is the inlet where the flow is uniform and the mixture fraction variation is given on the left. The lateral boundaries are periodic and represent the effects of confinement on the flame. The streamlines and reaction rate are shown within the domain. The inlet velocity, although always uniform, is adjusted to stabilize the flame within the domain.

periodic boundary conditions. This is in contrast to previous work on triple flames, which used nonreflecting boundary conditions in the lateral direction.

Within this domain we initialize the flow as a planar premixed flame, in which the mixture fraction, defined as

$$Z = \frac{1 + Y_F - Y_O}{2},$$

is everywhere equal to its stoichiometric value, $Z_{ST} = 0.5$. The incoming flow is uniform and set equal to the premixed laminar flame speed, S_L^0. Also associated with the flame is the premixed flame thickness, δ_L^0.

After the flow and flame are initialized, a sinusoidal perturbation is added to the uniform stoichiometric mixture fraction, specified by:

$$Z = Z_{ST} + \frac{\Delta Z}{2} \cos(2\pi y / L_{\Delta Z})$$

where $L_{\Delta Z}$ is the height of the domain in Fig. 1. In all cases, we maintain stoichiometric conditions on average. It should be noted that we are not dealing with a stability problem, in which a small perturbation is either damped or amplified. Rather, we introduce a finite disturbance in one field which produces finite changes

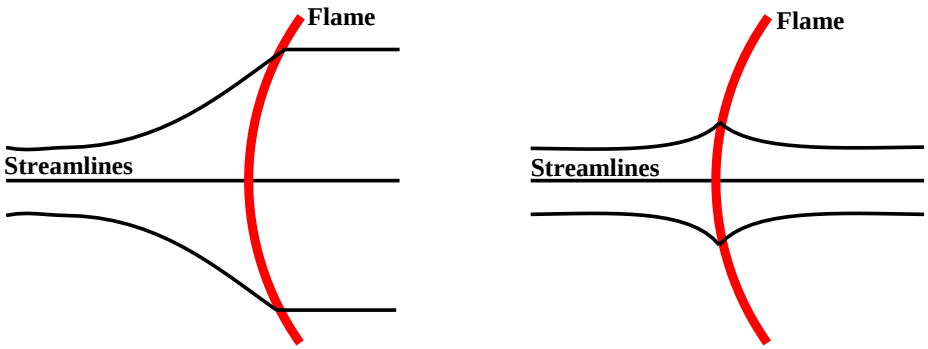

FIGURE 2. Streamline patterns for unconfined (left) and confined (right) flames. A redirection of the velocity vectors is observed across the flame front due to heat release effects. This redirection occurs upstream of the flame in the unconfined case, causing a divergence of the streamlines thus decelerating the horizontal velocity before the flame. As a result the propagation or upstream speed increases in order to maintain the premixed flames speed locally. In the confined case, the redirection of velocity vectors occurs both in front of and behind the flame. The increase in flame speed is much smaller in the confined cases and may be negligible for small wavelengths of lateral perturbations.

in the other fields. As this perturbation reaches the flame, the flame shape and propagation speed change, so the inlet velocity must be adjusted in order to achieve a steady-state solution. Because the variation in mixture fraction at the inlet has two stoichiometric points, two leading-edge flames occur. The range of mixture fraction is small enough, with $\Delta Z = 0.2$, that the diffusion flame is weak and is not apparent in the figure. In addition to the reaction rate, streamlines are also shown in the figure. Although we do observe streamline divergence in front of the flame, the propagation speed of the flame in Fig. 1, where $Le = 1$, remains equal to the planar premixed flame speed, S_L^0.

The use of periodic or confined rather than free lateral boundaries greatly affects the flame's propagation. For unconfined unity Lewis number flames, it has been shown that the ratio of the propagation speed relative to the plane laminar premixed flame varies with the square root of the density ratio across the flame. Depending on the wavelength of the mixture fraction perturbation in the confined case, this effect may be absent. A schematic representation of why this occurs presented in Fig. 2. In both cases, there is a redirection of velocity vectors across the flame front resulting from heat release effects. However, in the unconfined case this redirection occurs in front of the flame resulting in a strong divergence of streamlines in the unburnt region of the flow field. This divergence in streamlines results in a decrease in horizontal velocity prior to the flame. As a result, in order for the local flame speed to maintain a velocity equal to the premixed flame speed, the upstream or propagation speed must increase. In the confined case, the redirection of velocity vectors across the flame occurs both in front of and behind the flame, hence the increase in propagation speed is smaller than that of the unconfined case.

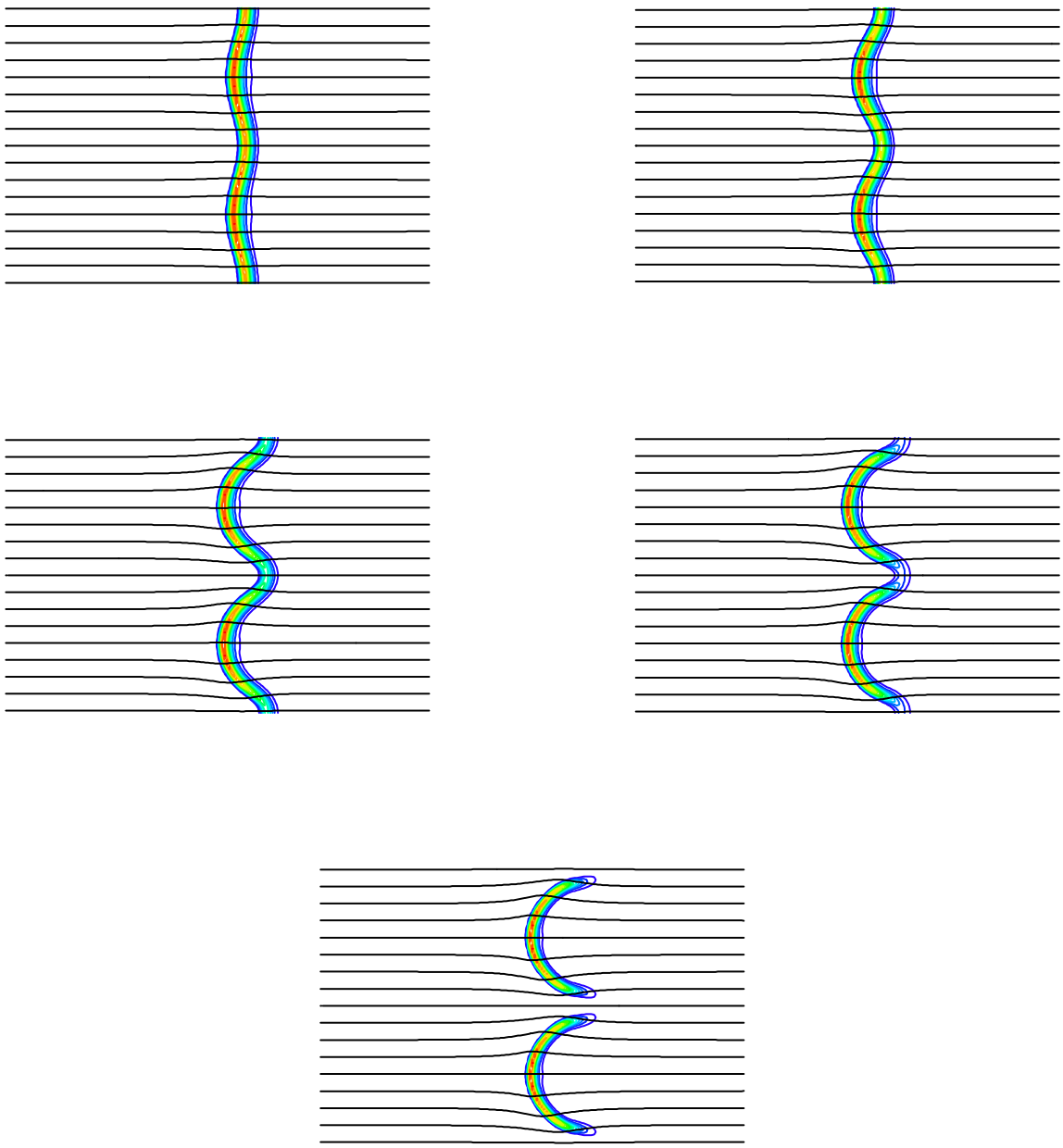

FIGURE 3. Reaction rate and streamlines for different Lewis number cases: $Le = 1.2$ top left, $Le = 1.0$ top right, $Le = 0.8$ center left, $Le = 0.6$ center right, and $Le = 0.4$ bottom. Flame surface area increases as the Lewis number becomes smaller. For the $Le = 0.4$ case, the flame trough opens due to leakage of reactants, similar to the case of a Bunsen flame.

2. Accomplishments

In this section we present results from simulations of nonunity Lewis number

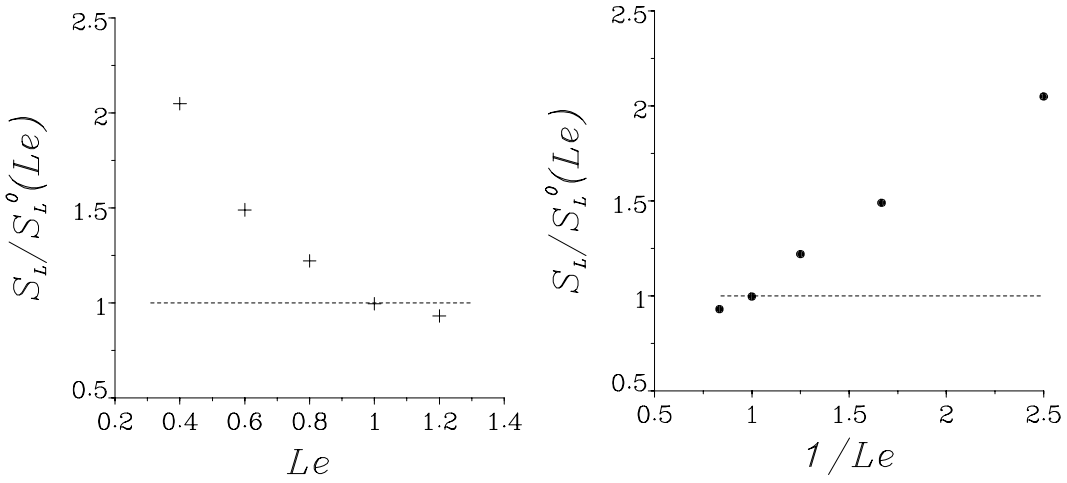

FIGURE 4. Flame speed as a function of Lewis number (left) and inverse Lewis number (right) Due to the strong confinement effects, the flame speed of the unity Lewis number case is that of the premixed flame speed. The flame speed increases with decreasing Lewis number, consistent with the thermal diffusive mechanism. Flame speeds are normalized by the planar premixed flame speed at stoichiometric conditions for the various Lewis numbers.

flames, followed by a discussion of a set of model equations used to analyze the flame's behavior. We start by discussing how the thermal-diffusive instability, in the context of partially premixed flames, modifies the flame shape.

The thermal-diffusive instability has been discussed thus far in terms of premixed flames. We now apply these concepts to our partially premixed case. The fundamental ideas mentioned above hold for the partially premixed case. In partially premixed combustion, however, the reaction rate is not constant along the flame front as in the premixed case. It is this gradient in reaction rate along the flame front that creates the perturbation in flame shape: the sections of the flame with mixture fractions closest to stoichiometry burn the fastest. Thus, to some degree the flame shape is determined by the approaching mixture fraction field. The thermal-diffusive mechanism then modifies this basic shape.

The modification of the basic flame shape due to the thermal diffusive mechanism is apparent from the flames in Fig. 3, where the reaction rate and streamlines are displayed for flames with Lewis numbers ranging from 0.4 to 1.2. Consistent with the thermal-diffusive mechanism, we observe that as the Lewis number decreases, the surface area of the flame increases. We should emphasize that the flame shapes in Fig. 3 are converged steady-state solutions. Although the thermal-diffusive instability accentuates the perturbation due to the variable mixture fraction field for Lewis numbers less than unity, the flame does reach a steady condition as nonlinear effects come into play (Williams 1996).

In addition to the modification of flame shape with Lewis number, we also observe an increase in flame speed, as shown in Fig. 4. The flame speed increases dramatically when the Lewis number drops below unity. We observe a flame speed more than twice the planar flame speed for $Le = 0.4$, which is larger than any flame

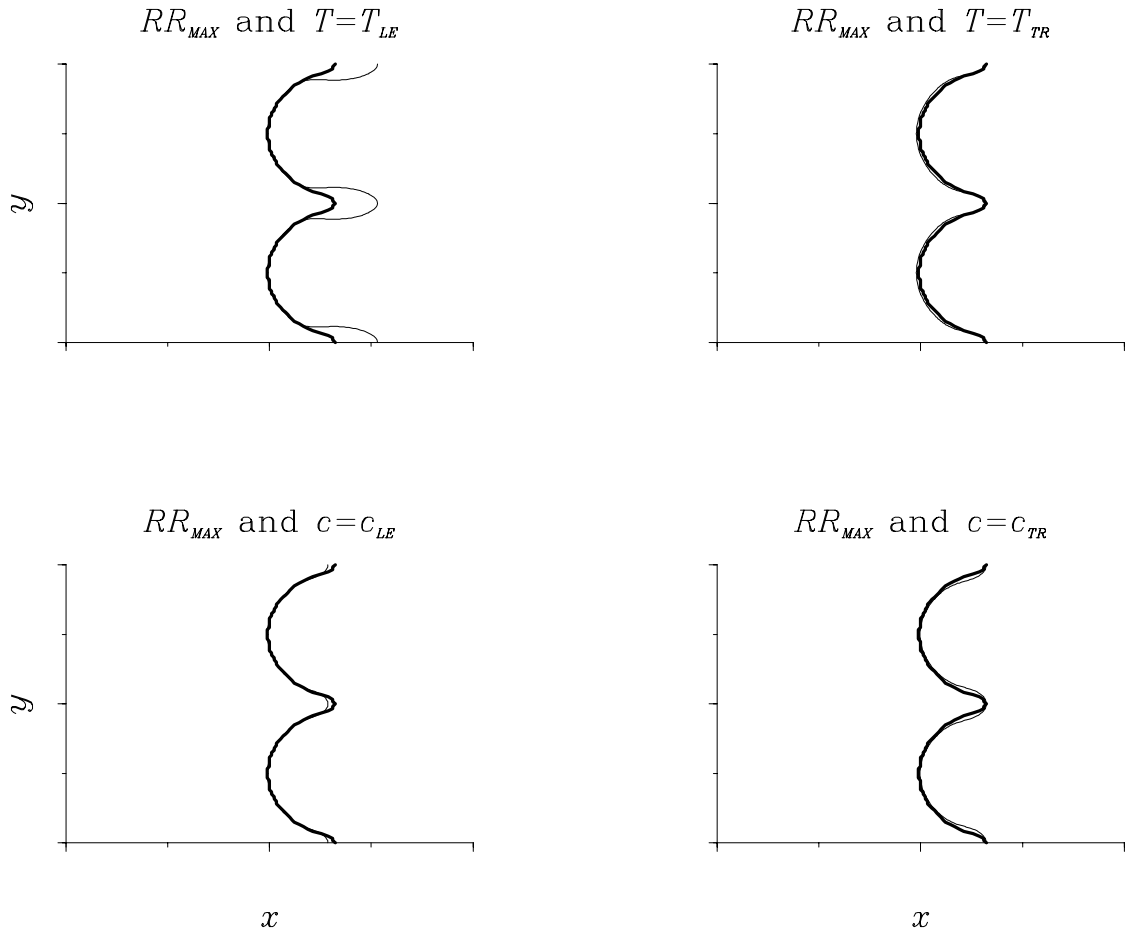

FIGURE 5. Flame surface (bold line), determined by maximum reaction rate on horizontal lines through the flame, and isocontours (thin line) of T and c for $Le = 0.4$ flames. Isovalues are T and c are chosen from the values along the flame surface at the leading edge (LE) and trough (TR). Although both fields have isocontours that track the flame surface reasonable well, the variable c is more reliable and is used as the progress variable.

speed observed in the unconfined configuration for $Le = 1$ flames (Ruetsch *et al.* 1995). One must also keep in mind that the mixture fraction range is $0.4 < Z < 0.6$ at the inlet and decreases before the mixture reaches the flame. Since the unconfined case has a much larger range in mixture fraction, $0 < Z < 1$, but produces a smaller increase in flame speed, it is evident that the Lewis number plays a strong role in the propagation characteristics of partially premixed flames. Also depicted in Fig. 4, we observe a good linear correlation of flame speed with the inverse of the Lewis number.

2.1 Progress variable

A necessary ingredient for further analysis of flame behavior is a definition of a progress variable which indicates the mixture's degree of reactedness. Together with the mixture fraction, the progress variable replaces the fuel and oxidizer mass fractions as independent variables. In premixed combustion, the progress variable

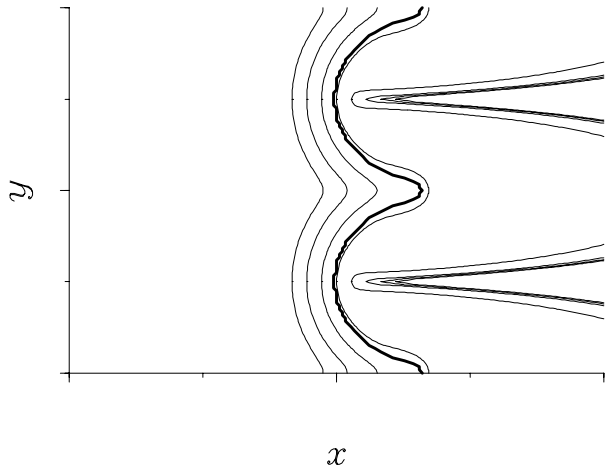

FIGURE 6. Flame surface (bold line) and various isovalue contours of the progress variable c. Before the premixed portion of the flame, the curvature of c and the flame surface are comparable. After the premixed flame, the radii of curvature of the c contours more closely resemble the thickness of the trailing diffusion flame.

can either be the reactant species mass fraction or the temperature. In partially premixed combustion, the issue is more complicated. We would like an isopleth of the progress variable to coincide with the flame surface. In partially premixed combustion, we define the flame surface as the curve connecting the horizontal extrema of the reaction rate. This curve is plotted in Fig. 5 for the $Le = 0.4$ flame along with temperature contours and the variable c given by:

$$c = 1 - Y_F - Y_O,$$

which is also the product mass fraction. The values of T and c used to obtain the isocontours are chosen to coincide with the flame surface at both the leading edge and trough.

From Fig. 5 we see that both quantities track the flame surface reasonably well. However, c follows the contour more closely, especially in the trough. We should point out that c reaches a value of unity only when neither fuel nor oxidizer are present. Therefore, in regions not at stoichiometric conditions, it is possible to burn one reactant completely and not have $c = 1$. In this respect, c does not have the traditional property of being unity when no further burning is possible. In spite of this shortcoming, we choose c as our progress variable for its ability to track the flame front and its linear dependence on the mass fractions of the reactant species.

The characteristics of c change considerably as we cross the flame surface, as indicated in Fig. 6. Prior to reaching the flame, the radius of curvature of c isocontours scale with the lateral thickness, $L_{\Delta Z}$. After passing through the flame surface, the radius of curvature scales with the thickness of the trailing diffusion flame. This has a large effect on the flame stretch, $\mathcal{K}$, defined as

$$\mathcal{K} = \nabla_T \cdot \mathbf{u} + S_L(Z)\kappa$$

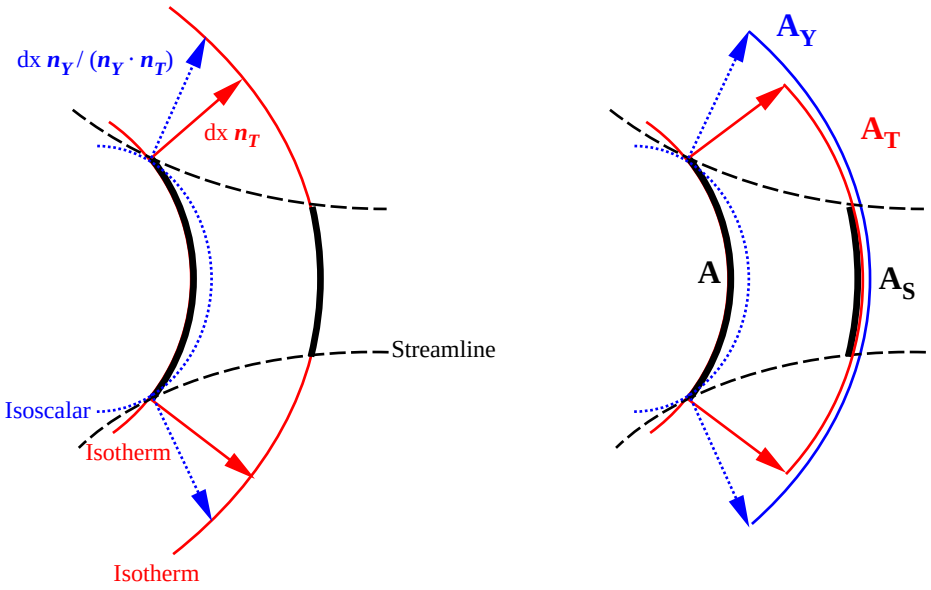

FIGURE 7. Control volumes for the one dimensional equation formulation. The control volume is bounded laterally by streamlines and by isotherms in the flow direction. The areas A_T and A_Y are used to define leakage of heat and species through the streamtube.

where ∇_T is the tangential gradient operator and $\kappa = \nabla_T \cdot \mathbf{n}_T$ is the curvature. Profiles of flame stretch through the flame surface indicate that stretch is dominated by curvature effects as expected and that no reasonable value can be assigned to the stretch as the change in the curvature through the flame is quite dramatic.

The inability to define a single value for curvature and thus flame stretch does not invalidate the use of c as a progress variable. One must remember that the concept of a progress variable strictly applies only to a premixed combustion. The fact that this quantity behaves differently in a region undergoing nonpremixed combustion does not invalidate its usefulness.

Because of the inability to define flame stretch accurately, the analysis of these partially premixed flames must proceed along an alternative path, which we discuss in the next section.

2.2 Model equations for partially premixed combustion

We now discuss a set of one-dimensional equations for analyzing the behavior of curved partially premixed flames. This method is based on the work of Echekki (1992) and Echekki (1996) for premixed combustion, which was used in analysis of the laminar flame tip by Poinsot *et al.* (1992). This approach reduces the Navier-Stokes equations to a set of one-dimensional equations while maintaining aspects of the flame's multidimensional nature through terms representing various isopleth curvatures. This approach differs from conventional models that handle the geometrical aspects exactly, while the physical processes are approximated. In our case, the terms representing the physical processes remain intact, and the geometrical aspects are approximated.

We begin by examining the control volume of Fig. 7, which is bounded laterally

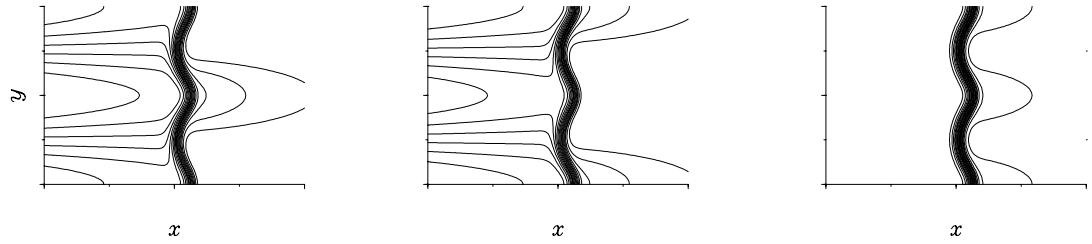

FIGURE 8. Fuel mass fraction (left), oxidizer mass fraction (center), and temperature (right) contour plots for $Le = 1$ case. For this partially premixed case, the need to account for a difference between the normals of the individual species and temperature fields is evident. The differences become stronger as one considers nonunity Lewis numbers and larger perturbations to the mixture fraction.

by streamlines and by isotherms in the streamwise direction. We define normals pointing in the flow direction for the temperature and various scalar fields as:

$$\mathbf{n}_T = \frac{\nabla T}{|\nabla T|}; \qquad \mathbf{n}_{Y_F} = -\frac{\nabla Y_F}{|\nabla Y_F|}; \qquad \mathbf{n}_{Y_O} = -\frac{\nabla Y_O}{|\nabla Y_O|}; \qquad \mathbf{n}_c = \frac{\nabla c}{|\nabla c|}$$

The distance between the two isotherms along the normal $\mathbf{n}_T$ is δx. We use the area of the first isotherm A as the base area, and define three surfaces along the second isotherm: the streamtube area, A_S; the area between the intersection of the two isotherm normals emanating from the boundaries of A with the second isotherm surface, A_T; and the area between the intersection of the two isoscalar normals, $\mathbf{n}_{Y_i}$, emanating from the boundaries of A with the second isotherm surface, A_Y. These latter two areas are used to account for the cross-stream diffusion of species and heat. The distance along $\mathbf{n}_{Y_i}$ between the two isotherm surfaces is given by:

$$\delta x_Y \mathbf{n}_{Y_i} = \frac{\delta x}{\mathbf{n}_{Y_i} \cdot \mathbf{n}_T} \mathbf{n}_{Y_i}.$$

This control volume differs from the one used by Echekki (1992) in that the normals to the isotherms and isopleths are not colinear. This is a necessity for partially premixed combustion, as demonstrated in Fig. 8, where contours of the fuel and oxidizer mass fractions, along with the temperature, are shown. It is desirable to use the progress variable c in place of the individual reactant species, and a transport equation for c is developed later in this paper. It suffices to mention here that $\mathbf{n}_c$ and $\mathbf{n}_T$ are not necessarily colinear, even for unity Lewis number. Figure 9 shows this clearly; $\mathbf{n}_c \cdot \mathbf{n}_T$ deviates from unity in the flame trough.

2.2.1 Area relations

In this section we develop relations between the reference areas A and A_S, used in defining our control volume, and the auxiliary areas A_T and A_{Y_i}, used in our analysis to account for cross-stream diffusion. A useful relation in obtaining such relations is the identity from Chung and Law (1988) in their integral analysis of stretched premixed flames:

$$A_2 = A_1(1 + \nabla_T \cdot \mathbf{a})$$

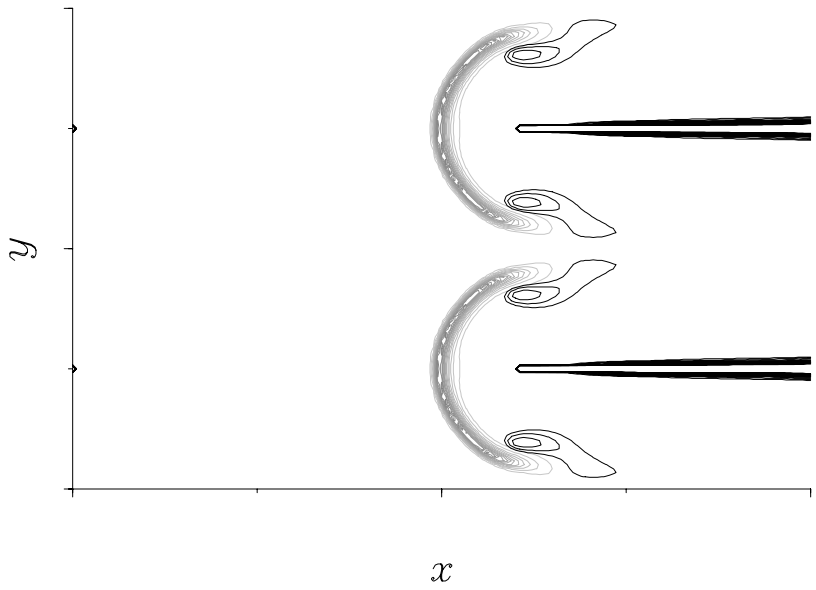

FIGURE 9. Alignment of progress variable and temperature normals for $Le = 0.4$ case. The reaction rate is shown in grey, and the dark contours show levels of $1 - \mathbf{n}_c \cdot \mathbf{n}_T$, thus departures from alignment. The greatest departure from alignment occurs in the trailing diffusion flame, but there are regions near the flame trough where the alignment of $\mathbf{n}_c$ and $\mathbf{n}_T$ is not preserved.

where $\mathbf{a}$ is any vector from a point on A_1 to A_2 and the gradient operator ∇_T represents the divergence on the plane tangent to A_1:

$$\nabla_T \cdot \mathbf{a} = \nabla \cdot \mathbf{a} - \mathbf{n}_T \mathbf{n}_T : \nabla \mathbf{a}$$

According to this relation we have:

$$A_T = A\left[1 + \delta x \nabla_T \cdot \mathbf{n}_T\right],$$

$$A_{Y_i} = A\left[1 + \delta x \nabla_T \cdot \left(\frac{\mathbf{n}_{Y_i}}{\mathbf{n}_{Y_i} \cdot \mathbf{n}_T}\right)\right],$$

and we express the streamtube area as

$$A_S = A + \delta A.$$

The term $\nabla_T \cdot \mathbf{n}_T$ is the curvature of the isotherm. The similar term in the equation for A_{Y_i} reduces to the isotherm curvature only if $\mathbf{n}_T = \mathbf{n}_{Y_i}$, in which case $A_T = A_{Y_i}$. We also define the differences between these areas as

$$\delta A_{TS} \equiv A_T - A_S = A\delta x \nabla_T \cdot \mathbf{n}_T - \delta A$$

and

$$\delta A_{Y_i S} \equiv A_Y - A_S = A\delta x \nabla_T \cdot \left(\frac{\mathbf{n}_{Y_i}}{\mathbf{n}_{Y_i} \cdot \mathbf{n}_T}\right) - \delta A$$

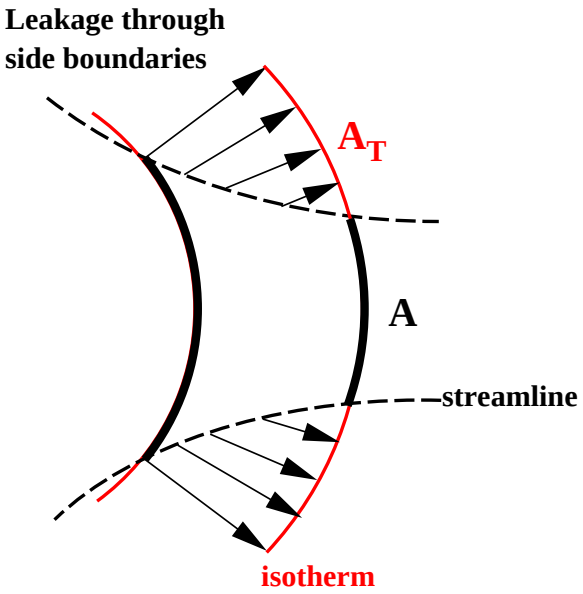

FIGURE 10. Lateral diffusion of heat through the streamtube. This leakage can be accounted for by measuring the flux through the expanded area in the downstream isotherm. (This diagram demonstrates the method used to account for thermal leakage, but the same concept applies to mass leakage through the streamtube.)

where in the limit of small δx we obtain:

$$\frac{dA_{TS}}{dx} = A\nabla_T \cdot \mathbf{n}_T - \frac{dA}{dx}$$

and

$$\frac{dA_{Y_i S}}{dx} = A\nabla_T \cdot \left(\frac{\mathbf{n}_{Y_i}}{\mathbf{n}_{Y_i} \cdot \mathbf{n}_T}\right) - \frac{dA}{dx}.$$

These relations provide a crucial link between the basic governing equations and our model equations. Since we are developing a set of one-dimensional equations, we need to include information regarding the other spatial dimensions. It is the behavior of the normal terms in these area relations that provide the multidimensional information required for adequate representation of the geometrical aspects of the problem.

2.2.2 Governing equations

With the area relations defined, we now consider conservation laws applied to the control volume. Since our control volume is bounded by streamlines, continuity is simply:

$$\delta[m] = 0$$

where m is the mass flow rate in the streamtube. The difference between values at the outlet and inlet isotherms is denoted as $\delta[\,] = [\,]_{x+\delta x} - [\,]_x$. The species equation is:

$$\delta[mY_i + \mathcal{M}_i] + \mathcal{F}_i \delta A_{Y_i S} = \dot{\omega}_{Y_i} \delta x A$$

where $\mathcal{M}_i = -\rho A \mathcal{D}_i dY_i/dx$, $\mathcal{F}_i = -\rho \mathcal{D}_i dY_i/dx$, and $\dot{\omega}_{Y_i}$ are the diffusive flow rate, diffusive flux, and rate of production of species i. The term $\mathcal{F}_i \delta A_{Y_i S}$ represents the leakage of species i across the streamtube, which is equivalent to the heat that crosses the area $\delta A_{Y_i S}$ as indicated in Fig. 10. In the limit of small δx this becomes:

$$m\frac{dY_i}{dx} + \frac{d\mathcal{M}_i}{dx} + \left[A\nabla_T \cdot \left(\frac{\mathbf{n}_{Y_i}}{\mathbf{n}_{Y_i}\cdot\mathbf{n}_T}\right) - \frac{dA}{dx}\right]\mathcal{F}_i = \dot{\omega}_{Y_i} A$$

or by substituting for $\mathcal{M}_i$ and $\mathcal{F}_i$:

$$m\frac{dY_i}{dx} - \frac{d}{dx}\left(\rho A \mathcal{D}_i \frac{dY_i}{dx}\right) - \rho\mathcal{D}_i\left[A\nabla_T \cdot \left(\frac{\mathbf{n}_{Y_i}}{\mathbf{n}_{Y_i}\cdot\mathbf{n}_T}\right) - \frac{dA}{dx}\right]\frac{dY_i}{dx} = \dot{\omega}_{Y_i} A \qquad (1)$$

The first and second terms in this equation represent the convection and diffusion processes across the isotherms. The term in square brackets, representing the leakage of reactants across the streamtube, contains information about the multidimensional nature of the flame.

Equation (1) can be used for each species so that, although this study uses a simple chemical scheme, the method can be applied to complex reaction mechanisms. In our case, we are more interested in the progress variable c and the mixture fraction Z than the mass fractions. We can obtain these equations by combining the equations for the individual species and substituting for c:

$$\begin{aligned} m\frac{dc}{dx} - \frac{d}{dx}\left(\rho A\mathcal{D}\frac{dc}{dx}\right) + \rho\mathcal{D}\frac{dA}{dx}\frac{dc}{dx} \\ + \rho\mathcal{D}A\left[\nabla_T\cdot\left(\frac{\mathbf{n}_{Y_F}}{\mathbf{n}_{Y_F}\cdot\mathbf{n}_T}\right)\frac{dY_F}{dx} + \nabla_T\cdot\left(\frac{\mathbf{n}_{Y_O}}{\mathbf{n}_{Y_O}\cdot\mathbf{n}_T}\right)\frac{dY_O}{dx}\right] = \dot{\omega}_c A \end{aligned}$$

where $\dot{\omega}_c = -(\dot{\omega}_{Y_F} + \dot{\omega}_{Y_O})$. To eliminate Y_F and Y_O from the equations, we use the relations

$$Y_F = Z - \frac{c}{2}; \qquad Y_O = 1 - Z - \frac{c}{2}$$

and obtain:

$$\begin{aligned} m\frac{dc}{dx} - \frac{d}{dx}\left(\rho A\mathcal{D}\frac{dc}{dx}\right) + \rho\mathcal{D}\left[\frac{dA}{dx}\frac{dc}{dx} + A\frac{dZ}{dx}\nabla_T\cdot\left(\frac{\mathbf{n}_{Y_F}}{\mathbf{n}_{Y_F}\cdot\mathbf{n}_T} - \frac{\mathbf{n}_{Y_O}}{\mathbf{n}_{Y_O}\cdot\mathbf{n}_T}\right)\right. \\ \left. - \frac{1}{2}A\frac{dc}{dx}\nabla_T\cdot\left(\frac{\mathbf{n}_{Y_F}}{\mathbf{n}_{Y_F}\cdot\mathbf{n}_T} + \frac{\mathbf{n}_{Y_O}}{\mathbf{n}_{Y_O}\cdot\mathbf{n}_T}\right)\right] = \dot{\omega}_c A. \end{aligned} \qquad (2)$$

In a similar fashion, we can develop an equation for Z:

$$\begin{aligned} m\frac{dZ}{dx} - \frac{d}{dx}\left(\rho A\mathcal{D}\frac{dZ}{dx}\right) + \frac{1}{2}\rho\mathcal{D}\left[2\frac{dA}{dx}\frac{dZ}{dx} + A\frac{dZ}{dx}\nabla_T\cdot\left(\frac{\mathbf{n}_{Y_F}}{\mathbf{n}_{Y_F}\cdot\mathbf{n}_T} + \frac{\mathbf{n}_{Y_O}}{\mathbf{n}_{Y_O}\cdot\mathbf{n}_T}\right)\right. \\ \left. - \frac{1}{2}A\frac{dc}{dx}\nabla_T\cdot\left(\frac{\mathbf{n}_{Y_F}}{\mathbf{n}_{Y_F}\cdot\mathbf{n}_T} - \frac{\mathbf{n}_{Y_O}}{\mathbf{n}_{Y_O}\cdot\mathbf{n}_T}\right)\right] = 0 \end{aligned} \qquad (3)$$

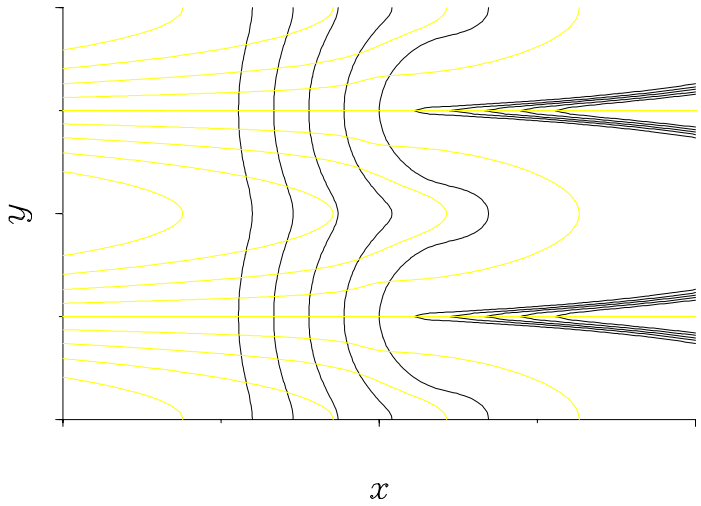

FIGURE 11. Alignment of progress variable and mixture fraction. Progress variable c (dark lines) and mixture fraction Z (grey scale) isopleths are shown for the $Le = 0.4$ case. Along the line through the leading edge $\mathbf{n}_c$ and $\mathbf{n}_Z$ are orthogonal; however, this is not the case as one moves from this line of symmetry.

Equation (2) clearly shows the effect of partial premixing on the evolution of the progress variable. To contrast Eq. (2) with the premixed case, we can write the evolution equation for c in premixed combustion for which $\mathbf{n}_{Y_F} = \mathbf{n}_{Y_O} = \mathbf{n}_T$, giving:

$$m\frac{dc}{dx} - \frac{d}{dx}\left(\rho A\mathcal{D}\frac{dc}{dx}\right) + \rho\mathcal{D}\frac{dc}{dx}\left[\frac{dA}{dx} - A\nabla_T\cdot\mathbf{n}_T\right] = \dot{\omega}_c A, \tag{4}$$

which is identical to the species equation of Echekki (1992). Equation (2) shows an explicit dependence on mixture fraction through the dZ/dx term, which modifies the equation when the isopleths of the fuel and oxidizer differ.

We have eliminated Y_F and Y_O in Eqs. (2) and (3), except for their implicit occurrence in the normal vectors. We can replace these by forming the normal vectors from our transformation equations:

$$\mathbf{n}_{Y_F} = \frac{\frac{1}{2}\nabla c - \nabla Z}{|\frac{1}{2}\nabla c - \nabla Z|}; \qquad \mathbf{n}_{Y_O} = \frac{\frac{1}{2}\nabla c + \nabla Z}{|\frac{1}{2}\nabla c + \nabla Z|} \tag{5}$$

Substitution of these quantities into Eqs. (2) and (3), in general, leads to complicated expressions but there are cases where simplifying assumptions can be made. These cases occur when the gradients of the progress variable and mixture fraction are either colinear or orthogonal.

In general, as demonstrated by Fig. 11, we cannot make assumptions about the alignment of $\mathbf{n}_c$ and $\mathbf{n}_Z$. However, along the line through the leading edge we find that $\mathbf{n}_c\cdot\mathbf{n}_Z = 0$. It is not sufficient that these normal vectors are orthogonal along this line of symmetry. Due to the ∇_T operator, we must also require that these normal vectors remain orthogonal as we move laterally. In cases where a substantial

region with $\mathbf{n}_c \cdot \mathbf{n}_Z \sim 0$ exists, the expressions in Eq. (5) simplify greatly. When $\mathbf{n}_c$ and $\mathbf{n}_T$ are collinear and $\mathbf{n}_Z$ and $\mathbf{n}_T$ are orthogonal, we can write:

$$\frac{\mathbf{n}_{Y_F}}{\mathbf{n}_{Y_F} \cdot \mathbf{n}_T} = \frac{\frac{1}{2}\nabla c - \nabla Z}{\frac{1}{2}\nabla c \cdot \mathbf{n}_T}; \qquad \frac{\mathbf{n}_{Y_O}}{\mathbf{n}_{Y_O} \cdot \mathbf{n}_T} = \frac{\frac{1}{2}\nabla c + \nabla Z}{\frac{1}{2}\nabla c \cdot \mathbf{n}_T}$$

Furthermore, along the leading edge streamtube $Z = 0.5$, thus $dZ/dx = 0$, which upon substitution in the conservation equation for c once again recovers the equation obtained for a premixed flame, which can be written as:

$$m\frac{dc}{dx} - A\left[\frac{d}{dx}\left(\rho\mathcal{D}\frac{dc}{dx}\right) + \rho\mathcal{D}\frac{dc}{dx}\nabla_T \cdot \mathbf{n}_c\right] = \dot{\omega}_c A. \tag{6}$$

We can determine the local streamwise velocity by manipulation of Eq. 6 to obtain:

$$u \sim \frac{m}{\rho A} = \mathcal{D}\left[\frac{d}{dx}\ln\left(\rho\mathcal{D}\frac{dc}{dx}\right) + \kappa + \frac{\dot{\omega}_c}{\rho\mathcal{D}dc/dx}\right]$$

where $\kappa = \nabla_T \cdot \mathbf{n}_T$ is the local curvature. The fact that we have a local curvature in this equation is desirable due to its rapid rate of change. It is instructive to contrast this equation with the multidimensional equation used in calculating the propagation velocity (Ruetsch and Broadwell 1995):

$$V = \frac{1}{\rho\left|\nabla c\right|}\frac{\partial}{\partial x_i}\left(\rho\mathcal{D}\frac{\partial c}{\partial x_i}\right) + \frac{1}{\rho\left|\nabla c\right|}\dot{\omega}_c.$$

The first term in the multidimensional equation corresponds to the first and second terms in the 1D equation, where the multidimensional diffusion term is broken up into streamwise and lateral, through curvature, components.

Through examination of Eq. (2) we have learned when partial premixing must be considered and under what circumstances the problem can be analyzed from a premixed standpoint: $\mathbf{n}_c \cdot \mathbf{n}_T = 1$ and $\mathbf{n}_c \cdot \mathbf{n}_Z = 0$ in a neighborhood of the streamtube. Under weak gradients of the mixture fraction, the leading edges of partially premixed flames to some degree fall in this category.

Up to this point, the issue of Lewis number effects has not been discussed in regards to the one-dimensional equations. In order for the Lewis number to come into play, we need to include both thermal and mass diffusion. Therefore, we look to energy conservation. The energy equation can be written in differential form as:

$$\delta\left[\sum_i (mY_i + \mathcal{M}_i)h_i + \mathcal{Q}\right] + \sum_i \delta A_{Y_i S}\mathcal{F}_i h_i + \delta A_{TS}\, q = \dot{\omega}_c Q_c A\delta x \tag{7}$$

where $\mathcal{Q} = -A\lambda dT/dx$, $q = -\lambda dT/dx$, and Q_c is the heat release from the chemical reaction per unit change in progress variable. The terms in brackets represent the flow of enthalpy across the isotherms due to convection and mass diffusion, as well

as heat conduction across the isotherms. The remaining terms represent the leakage of energy across the streamtube due to mass diffusion and heat conduction, along with heat release through chemical reactions. Defining $h = \sum Y_i h_i$ and assuming $h_i = h = c_p T$ for all i we have, after taking the limit of small δx:

$$m\frac{dT}{dx} - Le\frac{d}{dx}\left(\rho\mathcal{D}A\frac{dT}{dx}\right) - \rho\mathcal{D}T\sum_i \frac{dA_{Y_iS}}{dx}\frac{dY_i}{dx} - Le\rho\mathcal{D}\frac{dA_{TS}}{dx}\frac{dT}{dx} = \frac{Q_c}{c_p}\dot{\omega}_c A. \quad (8)$$

where we have represented all diffusion terms through the mass diffusion coefficient and use the Lewis number to effectively convert to the thermal diffusivity when required. After some manipulation, Eq. 8 becomes:

$$\begin{aligned} m\frac{dT}{dx} - Le\,A\left[\frac{d}{dx}\left(\rho\mathcal{D}\frac{dT}{dx}\right) + \rho\mathcal{D}\frac{dT}{dx}\nabla_T\cdot\mathbf{n}_T\right] \\ -\rho\mathcal{D}AT\left[\frac{dZ}{dx}\nabla_T\cdot\left(\frac{\mathbf{n}_{Y_F}}{\mathbf{n}_{Y_F}\cdot\mathbf{n}_T} - \frac{\mathbf{n}_{Y_O}}{\mathbf{n}_{Y_O}\cdot\mathbf{n}_T}\right)\right. \\ \left. +\frac{dc}{dx}\nabla_T\cdot\left(\frac{\mathbf{n}_c}{\mathbf{n}_c\cdot\mathbf{n}_T} - \frac{1}{2}\frac{\mathbf{n}_{Y_F}}{\mathbf{n}_{Y_F}\cdot\mathbf{n}_T} - \frac{1}{2}\frac{\mathbf{n}_{Y_O}}{\mathbf{n}_{Y_O}\cdot\mathbf{n}_T}\right)\right] = \frac{Q_c}{c_p}\dot{\omega}_c A. \end{aligned} \quad (9)$$

The first line of Eq. 9 contains the convective and thermal diffusion terms. The last two lines represent the energy change via mass diffusion through the lateral boundaries and the chemical source.

In the premixed limit, Eq. 9 reduces to:

$$m\frac{dT}{dx} - Le\,A\left[\frac{d}{dx}\left(\rho\mathcal{D}\frac{dT}{dx}\right) + \rho\mathcal{D}\frac{dT}{dx}\nabla_T\cdot\mathbf{n}_T\right] = \frac{Q_c}{c_p}\dot{\omega}_c A,$$

which holds not only in the premixed limit but also for the streamtube passing through the leading edge under the conditions used to obtain Eq. 6.

3. Future work

Up to this point, efforts have been concentrated on the development of the model equations described above. Future work will concern applying these equations to simulation data in order to determine the significance of certain processes and to obtain scaling behavior regarding flame propagation. In particular, we would like to recover the linear relation of flame speed with the inverse of the Lewis number depicted in Fig. 4.

One aspect of flame propagation that can be addressed using these equations is the process by which the flame trough is stabilized. The weak reaction rate and convergence of streamlines would suggest that the trough region doesn't stabilize, but simulations indicate that the flame does reach a steady state. Leakage of heat and species is evidently important in this region and can be analyzed using the model equations.

This laminar study allows one to develop an understanding of how fluctuations in the reactant composition alone affects flame behavior. Once the behavior of

these flames is understood, data from partially premixed turbulent simulations can be analyzed, where contributions from both velocity and mixture fraction fields modify flame behavior.

REFERENCES

Chung, S. H. and Law, C. K. 1988 An integral analysis of the structure and propagation of stretched premixed flames. *Combust. & Flame.* **72,** 325.

Dold, J. W. 1989 Flame propagation in a nonuniform mixture: analysis of a slowly varying triple flame. *Combust. & Flame.* **76,** 71.

Dold, J. W., Hartley, L. J., and Green, D. 1991 Dynamics of laminar triple-flamelet structures in non-premixed turbulent combustion. *Dynamical Issues in Combustion Theory.* Springer-Verlag, 83.

Echekki, T. 1992 Studies of curvature, strain, and unsteady effects on premixed flames. *Ph. D. Thesis,* Stanford University.

Echekki, T. 1996 A quasi-one dimensional premixed flame model with cross-stream diffusion. To appear in Combust. & Flame.

Hartley, L. J., and Dold, W. 1991 Flame propagation in a nonuniform mixture: analysis of a propagating triple-flame. *Comb. Sci. & Tech.* **80,** 23.

Kioni, P. N., Rogg, B., Bray, K. N. C., and Liñán, A. 1993 Flame spread in laminar mixing layers: the triple flame. *Combust. & Flame.* **95,** 276.

Lele, S. 1992 Compact finite difference schemes with spectral-like resolution. *J. Comp. Phys.* **103,** 16.

Müller, C. M., Brietbach, H., and Peters, N. 1994 Partially premixed turbulent flame propagation in jet flames. *25th International Symposium on Combustion.* p. 1099

Phillips, H. 1965 Flame in a buoyant methane layer. *10th International Symposium on Combustion.* p. 1277

Poinsot, T., and Lele, S. 1992 Boundary conditions for direct simulations of compressible viscous flows. *J. Comp. Phys.* **101,** 104.

Poinsot, T., Echekki, T., and Mungal, M. G. 1992 A study of the laminar flame tip and implications for premixed turbulent combustion. *Comb. Sci. & Tech.* **81,** 45.

Ruetsch, G. R., Vervisch, L., and Liñán, A. 1995 Effects of heat release on triple flames. *Phys. Fluids.* **7,** 1447.

Trouvé, A. 1991 Simulation of flame-turbulence interaction in premixed combustion. *Annual Research Briefs 1991.* CTR, Stanford University/Nasa Ames., 273-286.

Williams, F. A. *Combustion Theory* Addison-Wesley, NY, 1986.

Wray, A. A. Private communication.